



Multi objective optimisation of an electromagnetic valve actuator

Nicolas Bellegarde, Philippe Dessante, Jean-Claude Vannier, Pierre Vidal

► To cite this version:

Nicolas Bellegarde, Philippe Dessante, Jean-Claude Vannier, Pierre Vidal. Multi objective optimisation of an electromagnetic valve actuator. SENSACT 2007, Oct 2007, Gif-sur-Yvette, France. pp.1-6. hal-00222803

HAL Id: hal-00222803

<https://centralesupelec.hal.science/hal-00222803>

Submitted on 29 Jan 2008

HAL is a multi-disciplinary open access archive for the deposit and dissemination of scientific research documents, whether they are published or not. The documents may come from teaching and research institutions in France or abroad, or from public or private research centers.

L'archive ouverte pluridisciplinaire **HAL**, est destinée au dépôt et à la diffusion de documents scientifiques de niveau recherche, publiés ou non, émanant des établissements d'enseignement et de recherche français ou étrangers, des laboratoires publics ou privés.

Multi objective optimisation of an *electromagnetic* valve actuator

Nicolas BELLEGARDE, Jean-Claude VANNIER, Philippe DESSANTE, Pierre VIDAL

Supelec, Département Énergie, 3 rue Joliot-Curie 91192 Gif-sur-Yvette, France

Abstract: This paper is about a modelling and an optimisation of an electromechanical drive system. The device consists of a DC source, a power converter, a linear actuator and its load. The aim of the system is to drive a load along a linear displacement. The two main objectives are to reduce the actuator volume and the copper losses, which are contrary objectives. Here, we present an analytical modelling of the system and afterwards an optimisation of the linear actuator main dimensions in order to carry out the previous objectives.

Keywords: Linear actuator, variable reluctance, multi objective optimisation, copper losses, weight, volume.

1. Notations

a	Thickness of the mobile part (mm)
α	Slot's coefficient of occupation
b	Thickness of the bottom of the coil's slot (mm)
B_e, B_p	Flux density in the air gap and the mobile part (T)
d	Flow of the load (m^3/s)
e	Air gap (mm)
E	Power supply voltage (V)
F	Reference developed force (N)
f	Frequency (Hz)
h	Slot's height (mm)
H_e	Magnetic field in the air gap (A/m)
H_p	Magnetic field in the mobile part (A/m)
i, \hat{i}	Intensity in the coil and its maximum value (A)
J, J_{cond}	Current density in the slot and the conducting (A/mm^2)
ρ	Copper resistivity ($\Omega \cdot \text{m}$)
L_0	Coil's inductor (H)
M_a	Actuator weight (Kg)
n	Number of turns
P	Pressure (N/m^2)
P_J	Copper losses in the actuator (W)
R	Coil's resistance (Ω)
r_1	Internal radius of the actuator (mm)
r_2	Internal radius of the slot (mm)
r_3	External radius of the slot (mm)

r_4	External radius of the actuator (mm)
\Re_e	Air gap's reluctance (H^{-1})
\Re_f	Coil slot's reluctance (H^{-1})
S	Air gap's area (m^2)
s	Section of the load (m^2)
S_b	Coil's area (m^2)
T	Period (s)
τ	Duty cycle
v	Coil's voltage (V)
V_a	Volume of the actuator (m^3)
V_f	Volume of the magnetic part (m^3)
V_b	Volume of the coil (m^3)
V_p	Volume of the mobile part (m^3)
V_{sem}	Volume of the electronic components (m^3)
W	Maximum magnetic energy (J)
Ψ	Magnetic flux (Wb)

2. Introduction

A cross section of the linear actuator is given in figure 1.

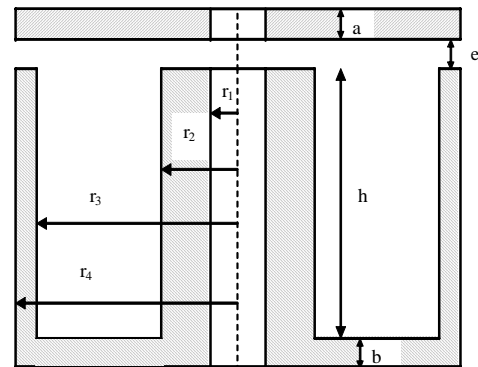


Figure 1 : Cross section of the actuator.

This actuator is a cylindrical structure the axis of which is represented by a dotted line.

It consists of two elements. The first element which is the smaller one, at the top of the figure, is the mobile part. It is a disc-shaped piece of magnetic material. This part is linked with a shaft which drives the mobile part of the load.

The second element, at the bottom of the figure, does not move. It is also made of magnetic material. A toric electrical coil takes place in the part located between radius r_2 and r_3 . The above mentioned shaft goes moving through the vertical hole situated in the centre of this second element.

When a current flows through the electrical coil, the mobile part of the actuator moves downwards. When the current stops, the mobile part goes upwards. This upwards displacement is due to the action of a spring.

3. System modelling

3.1 General relations for the linear actuator

Developed force on the axis:

$$F = \frac{B_e^2 \cdot S}{\mu_0} \quad (1)$$

Air gap's area:

$$S = \pi \cdot [r_2^2 - r_1^2] \quad (2)$$

This section can be also expressed by:

$$S = \pi \cdot [r_4^2 - r_3^2] \quad (3)$$

Coil's area:

$$S_b = [r_3 - r_2] \cdot h \quad (4)$$

Volume of the actuator:

$$V_a = \pi \cdot r_4^2 \cdot [h + a + b] \quad (5)$$

Volume of the coil:

$$V_b = \pi \cdot [r_3^2 - r_2^2] \cdot h \quad (6)$$

Volume of the magnetic part:

$$V_f = \pi \cdot r_4^2 \cdot [h + a + b] - V_b \quad (7)$$

Volume of the mobile part:

$$V_p = \pi \cdot r_4^2 \cdot h \quad (8)$$

Ampere law (first approximation):

$$ni = H_e \cdot [2h + r_3 - r_2] + 2 \cdot \frac{B_e}{\mu_0} \cdot e + H_p \cdot [r_3 - r_2] \quad (9)$$

Relation between the current density in the slot and the conducting:

$$J = \alpha \cdot J_{cond} \quad (10)$$

M.M.F. flowing through the coil:

$$ni = J \cdot h \cdot [r_3 - r_2] \quad (11)$$

3.2 General relations for the power converter

A simplified representation of the power converter is given in figure 2.

E is the power supply voltage. The actuator can be modelised by means of a resistance R in series with an inductance L .

When switches K_1 and K_2 are turned on, the current flows from the supply to the actuator. When they are turned off, the current can go down to zero through the diodes D_1 and D_2 .

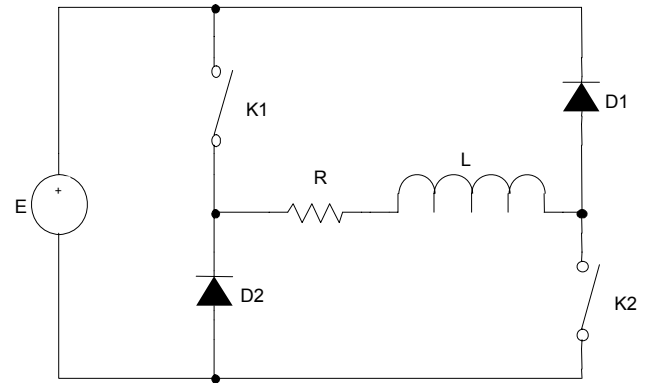


Figure 2 : Power converter.

The output current and voltage are given in figure 3.

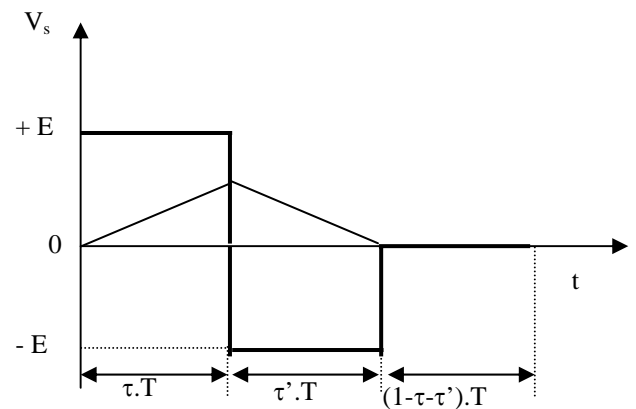


Figure 3 : Supply current and voltage.

The voltage v on the actuator's terminals is related to the current i and the magnetic flux Ψ according to the following equation:

$$v = R \cdot i + \frac{\partial \Psi}{\partial i} \cdot \frac{di}{dt} + \frac{\partial \Psi}{\partial x} \cdot \frac{dx}{dt} \quad (12)$$

The actuator is motionless when voltage is applied to it. The speed being equal to zero, equation (12) can be written as follows:

$$E = R \cdot i + L_0 \cdot \frac{di}{dt} \quad (13)$$

L_0 is equal to:

$$L_0 = n^2 \cdot \left[\frac{1}{\Re_e} + \frac{1}{\Re_f} \right] \quad (14)$$

The slot's reluctance is more important than the air gap's reluctance, thus we can write:

$$L_0 = n^2 \cdot \left[\frac{\mu_0 \cdot S}{2e} \right] \quad (15)$$

The resistive expression in equation (13) can be neglected. That leads to:

$$E = n \cdot \left[\frac{\mu_0 \cdot S}{2e} \right] \cdot \frac{d(ni)}{dt} \quad (16)$$

Considering time related linear variations, equation (16) becomes:

$$E = n \cdot \frac{B \cdot S}{\tau T} \quad (17)$$

The volume of the electronic components V_{sem} varies in a same way as the product of maximal current and voltage.

At last, it can be written:

$$V_{sem} \propto E \cdot \hat{i} = \frac{1}{\tau T} \cdot \frac{B_e^2 \cdot S}{\mu_0} \cdot 2e \quad (18)$$

Or again:

$$V_{sem} \propto E \cdot \hat{i} = \frac{2}{\tau T} \cdot F \cdot e \quad (19)$$

3.3 General relations for the load:

The flow d of the load is given by:

$$d = e \cdot s \cdot f \quad (20)$$

The required force F is equal to:

$$F = P \cdot s \quad (21)$$

The mechanical power is given by:

$$F \cdot e \cdot f = d \cdot P \quad (22)$$

So, d and P given, we can write:

$$F = \frac{d \cdot P}{e \cdot f} \quad (23)$$

F decreases while e and f increase. A compromise must be done taking into account the usual values of the working frequencies utilised for electromechanical actuators and their associated power converters.

4. System optimisation

4.1 General relations for the optimisation

The working of the actuator is ruled by the following relations.

Developed force:

$$F = \frac{B_e^2 \cdot S}{\mu_0} \quad (24)$$

Relation between fluxes in the air gap and the mobile part:

$$B_e \cdot S = B_p \cdot [2\pi \cdot r_2 \cdot a] \quad (25)$$

Flux relations in the bottom of the slot (no leakage):

$$2\pi \cdot r_2 \cdot b \cdot B_e = B_e \cdot S \quad (26)$$

Equality of the two air gap's areas:

$$S = \pi \cdot [r_2^2 - r_1^2] = \pi \cdot [r_4^2 - r_3^2] \quad (27)$$

Ampere law and M.M.F. definition:

$$J \cdot h \cdot [r_3 - r_2] = H_e \cdot [2h + r_3 - r_2] + 2 \cdot \frac{B_e}{\mu_0} \cdot e + H_p \cdot [r_3 - r_2] \quad (28)$$

Finally, we can note there are five independent relations.

4.2 Objective functions

Depending on the application, different cost functions can be minimized. Here, we present an optimisation where the actuator volume and the copper losses are the cost functions.

We can express the actuator volume as follows:

$$V_a = \pi \cdot r_4^2 \cdot [h + a + b] \quad (29)$$

Concerning the copper losses, it comes:

$$P_J = \frac{\rho \cdot V_b \cdot J^2}{\alpha} \quad (30)$$

With relation (6), we obtain:

$$P_J = \rho \cdot \pi \cdot \frac{h \cdot [r_3^2 - r_2^2] \cdot J^2}{\alpha} \quad (31)$$

Where ρ is the copper resistivity.

4.3 Parameters

There are eight geometrical parameters:

$$r_1, r_2, r_3, r_4, a, b, h, e$$

two magnetic parameters:

$$B_e, B_p$$

one electrical and one mechanical parameter:

$$J \text{ and } F$$

This leads to 12 parameters.

Working requirements: r_1 is assigned by the size of the shaft which drives the load. Nevertheless, we can notice the whole volume decreases while this radius decreases. The required force F and the air gap e are given by the working conditions. Thus, the values of those three parameters are known.

The value of the flux density in the magnetic material (fixed part) depends on the material's characteristic. Figure 4 shows the characteristic $B_e(H_e)$ used for the rest of the study.

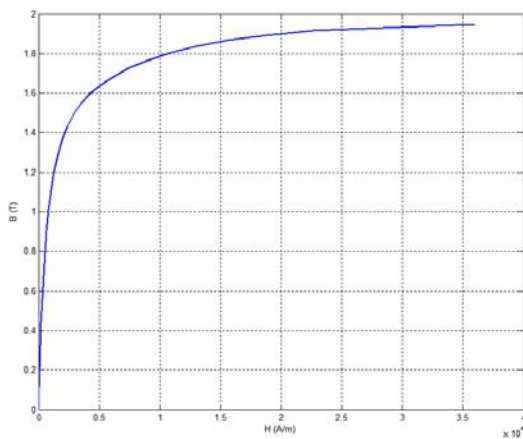


Figure 4 : Material's characteristic $B_e(H_e)$.

Concerning the flux density in the mobile part, we'll take a constant value among the following:

$$B_p = \begin{pmatrix} 0,5 \\ 1 \\ 1,5 \\ 2 \end{pmatrix} T \quad (32)$$

At last, only eight parameters are independent:

$$r_2, r_3, r_4, a, b, h, B_e, J$$

Finally, five relations and eight parameters lead to a three degrees of freedom system.

4.4 Constraints

In this application, two types of constraints are considered: the physical constraints which ensure that the linear actuator can supply load requirements and the geometrical constraints which permit to define a feasible motor.

Concerning the physical constraints, the following will be used:

$$F = 500 N \quad (33)$$

$$3 A/mm^2 \leq J \leq 15 A/mm^2 \quad (34)$$

$$\alpha = 0,7 \quad (35)$$

The geometrical constraints are given by these relations:

$$r_1 = 7 mm \quad (36)$$

$$e = 1,2 mm \quad (37)$$

$$r_2 > r_1 + 2 mm \quad (38)$$

$$r_3 > r_2 + 2 mm \quad (39)$$

$$50 mm \geq r_4 > r_3 + 2 mm \quad (40)$$

$$1 mm \leq a \leq 20 mm \quad (41)$$

$$1 mm \leq b \leq 20 mm \quad (42)$$

$$10 mm \leq h \leq 100 mm \quad (43)$$

5. Results

We present here the results concerning the definition of the linear actuator for a given load whose characteristics were given in the previous paragraph.

The optimisation procedures use the constraints (33-43) and searches a set of values for $r_2, r_3, r_4, a, b, h, B_e, J$ which minimises the considered cost function given by (29) or (31). The optimisation is made with Mathematica and verified with Matlab and a home made genetic algorithm.

Table 1 gives results obtained when the copper losses are the cost function (here we take $B_p = 1 T$).

$r_2 = 34,3 \text{ mm}$	$r_3 = 37,1 \text{ mm}$
$r_4 = 50 \text{ mm}$	$h = 99,5 \text{ mm}$
$a = 6,9 \text{ mm}$	$b = 16,4 \text{ mm}$
$B_e = 0,42 \text{ T}$	$J = 3 \text{ A/mm}^2$
$V_a = 965 \text{ cm}^3$	$P_J = 14 \text{ W}$

Table 1 : Minimisation of the copper losses ($B_p = 1 T$).

Table 2 gives results obtained when the volume of the actuator is the cost function (here again we have $B_p = 1 T$).

$r_2 = 11,6 \text{ mm}$	$r_3 = 20,2 \text{ mm}$
$r_4 = 22,2 \text{ mm}$	$h = 24,2 \text{ mm}$
$a = 5,6 \text{ mm}$	$b = 3,7 \text{ mm}$
$B_e = 1,54 \text{ T}$	$J = 15 \text{ A/mm}^2$
$V_a = 52 \text{ cm}^3$	$P_J = 115 \text{ W}$

Table 2 : Minimisation of the actuator volume ($B_p = 1 T$).

We can see that the volume and the losses in an actuator are contrary objectives. Indeed, figure 5 shows Pareto Front associated with the problem.

When the copper losses are the objective function, the reduction of these losses implies an increase of the coil's area and then an increase of the actuator volume.

On the other way, when the actuator volume is the objective function, the reduction of this volume implies an increase of the current density in the coil and then an increase of the copper losses.

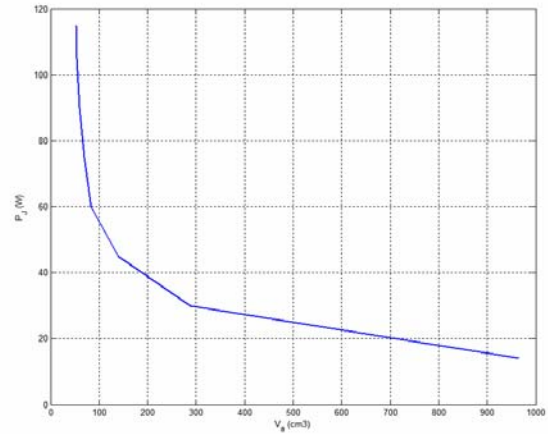


Figure 5 : Pareto Front ($B_p = 1 T$).

The following figures (6-7) shows the flux density influence in the mobile part. Figure 6 concerns the optimisation of the copper losses and figure 7 is about the minimisation of the actuator volume.

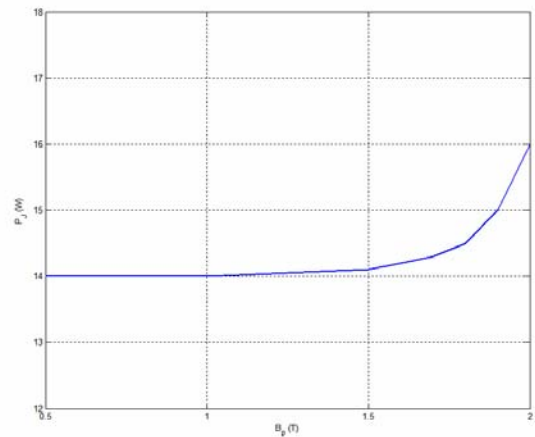


Figure 6 : Copper losses in function of B_p .

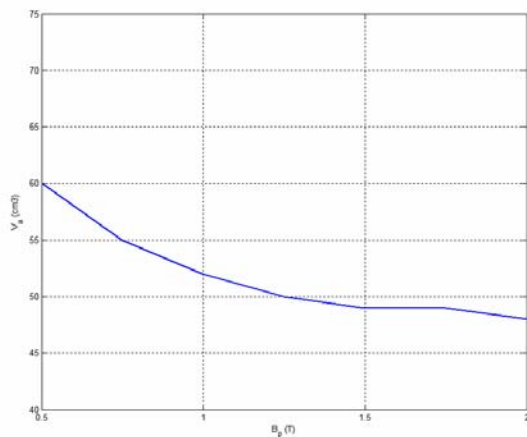


Figure 7 : Actuator volume in function of B_p .

We can see, in consideration with the scale, that the influence of the flux density in the mobile part is minimal.

However, an increase of the flux density in the mobile part implies a diminution of the associated thickness, and then a volume decrease. On the contrary, this flux density increase implies a growth of the copper losses.

6. Conclusion

In this paper, the volume and the copper losses of an electromechanical conversion system has been optimised. Firstly, a model of a linear actuator has been done. This model links the motor main dimensions to its performances. Then, the actuator volume and the copper losses in the coil have been written in function of the optimisation parameters. Secondly, an optimisation procedure was executed in order to minimise these objective functions. Different numerical optimisation methods were used to valid the methodology. All gave the same results. Finally, we can note that the losses and the volume are contrary objectives: when the copper losses are minimised ($P_J = 14 \text{ W}$), the actuator volume is maximum ($V_a = 965 \text{ cm}^3$); on the contrary, when the actuator volume is optimised ($V_a = 52 \text{ cm}^3$), the copper losses are maximum ($P_J = 115 \text{ W}$).

7. References

- [1] C. ESPANET, J. BIGEON: "Utilisation de l'optimisation pour rénover l'enseignement de la conception des machines électriques – Description d'un travail pratique utilisant le logiciel Pro@Design", CETSIS'2005, Nancy, France, 2005.
- [2] M. KADIRI, D. VALETTE, J.-C. VANNIER: "Fast electromechanical actuator with linear displacement", Proc of 6th international conference on optimisation of electrical and electronic equipment, p87, Brasov, Roumanie, 1998.
- [3] A. ARZANDÉ, F. DUGUÉ, J.-C. VANNIER, P. VIDAL: "Actionneur électrique rapide de pompe à carburant : modélisation, simulation dynamique et système de commande", Aerospace Energetic Equipment, Avignon, France, 2002.
- [4] F. DUGUÉ, B. BONAFOS, J.-C. VANNIER, P. VIDAL: "Actionneur linéaire rapide, conception, simulation et essais", EF2001, Nancy, France, 2001.
- [5] J.-C. VANNIER, P. VIDAL: "Analyse et modélisation d'un moteur à reluctance variable à circuit magnétique", EF99, Lille, France, 1999.
- [6] D. DE SAVIGNY: "Electroaimants de Commande", Techniques de l'Ingénieur, Volume D, pp. 835_1-837_14.
- [7] N. BELLEGARDE, P. DESSANTE, P. VIDAL, J.-C. VANNIER: "Optimisation of a drive system and its epicyclic gear set", ISEF2007, Prague, Czech Republic, 2007.
- [8] F. MATSUMARA, S. TACHIMORI: "Magnetic Suspension System Suitable for Wide Range Operation", EE in Japan, Volume 99, No.1, pp. 29-35, 1979

8. Glossary

MMF: Magneto-motive force